Computational screening approaches for investigating potential activity of phytoligands against SARS-CoV-2

Acharya Balkrishna
Patanjali Research Institute
Pallavi Thakur
Patanjali Research Institute
Shivam Singh
Patanjali Research Institute
Swami Narsingh
Patanjali Research Institute
Namita Singh
Guru Jambheshwar University of Science and Technology
Rakesh Kumar Sharma (rksharmadrl@yahoo.com)
Saveetha Institute of Medical and Technical Sciences

Research Article

Keywords: Corona virus, COVID-19, Drug designing, Herbal drug, Molecular docking, SARS-CoV-2

Posted Date: April 16th, 2020

DOI: https://doi.org/10.21203/rs.3.rs-23206/v1

Abstract

Objective: SARS-CoV-2 causes COVID-19, a life-threatening respiratory illness with high rates of morbidity and mortality. As on date, there is no specific medicine to prevent or treat COVID-19. Therefore, there is an acute need to identify evidence-based holistic and safe mitigators.

Methods: The present study is aimed to screen ligands of herbal origin using rationale based bioprospection analysis and subsequently predict their binding potential subdue the major drug targets for novel Coronavirus by employing computer-aided virtual screening. Further, comparative analysis of the binding potential of an approved chemical analogue and selected herbal ligands were also predicted. The selection of receptors was performed based on their pathophysiological relevance, as assessed by a PubMed based keyword hits matrix analysis. The drug likeliness and ADMETox descriptors of 24 herbal ligands were computationally predicted. Docking studies were further conducted with those phytoligands that qualified these parameters. An existing antimalarial drug, hydroxychloroquine, was also docked with all the selected viral receptors and its theoretical binding energy was set up as a standard for comparison as well as scrutinization of binding energies of the phytoligands.

Results: The docking studies suggested that the herbal ligand, namely, gamma-glutamyl-S-allylcysteine demonstrated highly significant binding energies with viral spike glycoprotein, endoribonuclease and main protease (binding energy ≥ -490 kcal/mol for all the tested viral receptors).

Conclusion: Gamma-glutamyl-S-allylcysteine demonstrated more significant binding potential as compared to the known chemical analogue, *i.e.*, hydroxychloroquine, as observed in the computational docking studies. This study serves to present pre-eminent information for further clinical studies highlighting the utility of herbal ligands as probable lead molecules for mitigating novel Coronavirus infection.

1. Introduction

Coronaviruses (CoVs) represent a category of infectious agents, belonging to the family Coronaviridae, categorized into four genera, namely, alpha-CoV, beta-CoV, gamma-CoV, and delta-CoV along with their subclasses (Lefkowitz et al., 2018). These CoVs contain large host-derived membrane envelope, helical nucleocapsid, non-structural proteins (nsp 1–16) and positive sense, single-stranded RNA (~ 26–32 kilobases). The viral RNA is capable enough of initiating infection within the host, even without the presence of essential enzymes (Tripp & Tompkins, 2018). Since the beginning of the 21st century, CoVs have caused three zoonotic outbursts, namely, severe acute respiratory syndrome (SARS-CoV; 2002–2003), Middle East respiratory syndrome (MERS-CoV; 2012), and the COVID–19, caused by severe acute respiratory syndrome Coronavirus 2 (SARS-CoV–2; 2019) (Zaki et al., 2012; Ou et al., 2020). The novel COVID–19 pandemic originated from the Hubei province of Central China during the late November, 2020, with its epicenter being in Wuhan city harbouring nearly 11 million people (Hu et al., 2020). This infection has been growing since then and has spread to more than 205 countries (Cucinotta & Vanelli, 2020; WHO, 2020). The transmissibility and penetrance rate of this infection is frequently changing at hourly and daily basis (Roser et al., 2020).The clinical manifestations of the novel COVID–19 infection include respiratory, gastrointestinal, nephrological and neurological etiologies (Balkrishna et al., 2020). Primary transmission of this infection involved zoonotic spread from animals (possibly bats) to humans (Zhang et al., 2020; Zhou et al., 2020). In particular, the primary transmission of COVID–19 infection was apparently linked to the ingestion of live animal and seafood (Balkrishna et al., 2020). Although the bat CoV bears maximum similarity with SARS-CoV–2, but due to the difference in specific

amino acid residues, the bat CoV could not directly infect humans, nevertheless there would be an intermediate host between bats and humans for the transmittance of the virus (Cyranoski, 2020). Subsequently, secondary transmission occurred among humans, leading to a faster rate of spread of the infection within the community (Guan et al., 2003; Balkrishna et al., 2020). The incubation period of SARS-CoV–2 ranges between 1–14 days with the median incubation period of about 5 days. An infected person will apparently show symptoms after the median incubation period. However, the infected individual can spread the infection since contracting the disease. The primary mode of transmission of COVID–19 infection is through contact with the infected individuals and/or by respiratory droplets (Carlos et al., 2020). Some studies have also proposed that SARS-CoV–2 may also propagate by the faecal shredding of infected or even cured individuals (Yeo et al., 2020).

The COVID–19 infection has become a global health challenge owing to its high morbidity (~3.17%); transmission rate (~2.2 per patient) (Sun et al., 2020); longer half-life of virus (~4–72 hours); and asymptomatic mode of transmission (~2–14 days of incubation) (Huang et al., 2020; Balkrishna et al., 2020).The most common indications of COVID–19 comprise of fever, nasopharyngeal congestion, dry cough, sore throat, dyspnoea, diarrhoea, neurological disorders and multiple organ failure. However, some patients act as asymptomatic carriers of the disease which are most difficult to diagnose and consequently treat. Even though the distinct symptoms seem to be mild, but can rapidly enhance to severe conditions, and even death (Huang et al., 2020; Kim, 2020).

The exact molecular pathogenesis of SARS-CoV–2 is yet not known with certainty; however, it has been proposed that viral pathogenesis is triggered by the release of proinflammatory cytokines that are associated with the activation of several signaling pathways, namely, TLRs-dependent IFN induction pathways (IRF–3/7& NF-Kβ) and myeloid-differentiation primary response 88 pathways (ATF–2 & AP–1). The primary virulence factors of the virus include SARS-CoV–2 spike glycoprotein (viral envelope protein responsible for viral attachment and entry within the host cells); viral nuclease (NSP15 endoribonuclease responsible for mediating viral capsid formation); and protease (Main Protease 3CLpro responsible for viral capsid formation) (Chen et al., 2020). SARS-CoV–2 mainly targets the alveolar and bronchial epithelial cells. The viral spike glycoprotein interacts with the ACE–2 receptors of the host cell, thereby mediating the viral entry. Afterwards, there occurs an elevated release of proinflammatory cytokines (IL–6 and IL–12), chemokines (IL–8, CCL–2 and CXCL10) and interferon. The virus gets hold of the host cell machinery and manipulates it for driving the process of viral replication. Virus also attempts to inhibit the production of interferon and proinflammatory cytokines by means of RNA helicases and non-structural proteins (Nsp 1, 3, 7 & 15). Subsequently, the viral load keeps on rising within the host system, ultimately leading to viraemia (*Figure 1)*.. Meanwhile, the host immune system also strives to fight back. The further spread of virus within the host system depends on the immunological status of the host. Immunomodulatory remedies play a pivotal role at this phase, wherein such moieties may mediate the transformation of an immunocompromised individual to an immunocompetent one.

Although, the structure and sequence of SARS-CoV–2 have been identified and drug screening followed by clinical trials are continuously being conducted by targeting these virulence factors. However, there are no approved drugs for effectively managing COVID–19 infection, probably due to unidentified dynamic pathophysiology; high mutagenicity of the virus; and adverse side effects of earlier known Coronavirus vaccines and drugs (Guo et al., 2020; Senathilake et al., 2020; Wang et al., 2020). In light of the outbreak, several treatment regimes have been proposed, including traditional medicinal moieties, that have been extensively used during the former epidemic outbreaks, such as SARS and H1N1 influenza (Zakaryan et al., 2017; Guerriero et al., 2018; Yang et al., 2018; Ang et al., 2020; Jo et al., 2020). Herbals provide a unique solution in terms of their negligible side effects, synergistic activity, broad spectrum therapeutic ability and immunomodulation effects (Thakur et al., 2016).

In the present study, the drug-like potential of secondary metabolites of herbal origin will be studied by targeting SARS-CoV–2 spike glycoprotein (S2), viral nuclease (NSP15 endoribonuclease) and protease (Main Protease 3CLpro). The selection of herbal secondary metabolites is based on investigating the potency of various herbals showing resistance towards viral virulence factors as indicated by various scientific search engines based on priority indexing. All the selected herbal moieties were subjected to molecular docking using Hex software, so as to assess the interactions of phytoligands with the viral receptors. Further screening of the propitious herbal leads was conducted by assessing the *in silico* toxicity and Lipinski score based drug likeliness. Bulk outliers showing high toxicity/mutagenicity or violating the Lipinski rules were eliminated. Subsequently, the drug-receptor interaction of the filtered herbal moieties was studied so as to obtain a lead molecule which could be further tested at preclinical and clinical levels. Although search for potential leads targeting the novel Coronavirus will continue perpetually, but these herbal leads may serve to be highly beneficial owing to their antiviral activities, potentiating nature and symptomatic relief provision capabilities, presented along with limited toxicities and comprehensive treatment strategy.

2. Materials And Methods

2.1 Selection and preparation of viral virulence factors as receptors

The receptors were selected based on their role in causing viral infection by SARS-CoV–2 virus. These receptors were assigned a weightage score on the basis of their pathophysiological relevance. Such pertinence was assessed by conducting a keyword hits scoring matrix using PubMed search engine. The random keyword search was conducted using combination keyword as ‘virulence factor inhibition + antiviral activity’. The first 20 hits provided by the search engine, working on the principle of priority indexing, were based on the number of times a website is clicked (Qin et al., 2005). This sample set based analysis was used to evaluate the net weightage linked to each virulence factor, using the following formula:

$$\%\ \text{Relevance index} = \frac{\text{No. of relevant hits based on observational analysis} * 100}{\text{Total No. of hits screened } (\sim n=20)} \ldots \textbf{(Eq. 1)}$$

The crystal structures of the selected relevant protein targets, namely, SARS-CoV–2 spike glycoprotein (S2; PDB code: 6VSB), viral nuclease (NSP15 endoribonuclease; PDB code: 6VWW) and protease (Main Protease 3CLpro; PDB code: 1Q2W) were obtained from RCSB Protein Data Bank (https://www.rcsb.org/). These structures were examined critically using Ramachandran Plot by ProCheck so as to validate the modeled protein structures based on the φ (phi), ψ (psi) and ω (omega) angles, thereby inspecting the quality of the target protein structures selected for docking studies. Furthermore, hydrogen atoms were introduced in all these 3D structures using Argus Lab (4.0.1), so as to customize the viral receptors for rigid docking (http://www.arguslab.com/arguslab.com/ArgusLab.html).

2.2 Active site analysis of viral virulence factors

The prediction of active sites of viral receptors was accomplished by DoG Site Scorer, and the Cartesian coordinates x, y, z (active sites) for effective docking were visualized in Argus Lab. These regions were further used for the generation of grid box for docking studies by Hex Cuda 8.0.0. Predictions with DoG Site Scorer were based on the difference of Gaussian filter to detect potential pockets on the protein surfaces and thereby splitting them into various sub-pockets. Subsequently, global properties, describing the size, shape and chemical features of the predicted pockets were calculated so as to estimate simple score for each pocket, based on a linear combination of three descriptors, *i.e.,*, volume, hydrophobicity and enclosure. For each queried input structure, a druggability score between 0-to–1 was obtained. Higher the druggability score, higher the physiological relevance of the pocket as

potential target. The active sites with best druggability scores were envisaged as an essential requirement for the creation of grid in selected viral receptors (Volkamer et al., 2012).

2.3 Selection and preparation of herbals as promising anti-SARS-CoV–2 candidates

A total of 24 bioactive compounds from naturally available medicinal plants were selected by employing a biostatistical matrix based analysis. Based on the understanding of the pathophysiological targets of the novel Coronavirus, herbal candidates exhibiting inhibitory properties specific to the viral virulence factors were searched in the PubMed repository. The descriptors used for conducting PubMed search with the help of extensive literature surge included keywords as 'virulence factor inhibition + herbal moiety'. Binary coefficient for the herbal moieties were calculated by assessing the presence or absence of particular inhibiting property exhibited against individual physiological target. The binary score for each plant ranged from 0 to 6, wherein the median cut-off value was selected as 3. Plants having a binary score ≥ 3 were considered for further weightage based matrix analysis, wherein the binary score of each plant was multiplied with the relevance score of the viral virulence factor (Refer to Section 2.1). Ultimately, a fuzzy set membership analysis was conducted in order to obtain a universal score for each plant. The fuzzy set score ranged between 0 and 1, wherein the plants with a fuzzy score greater than 0.5 were further selected for assessing their specific anti-SARS-CoV–2 activity.

$$\mu S = \frac{S - \min S}{\max S - \min S} \ldots \textbf{(Eq. 2)}$$

where, μS represents the desirability values of members of the fuzzy set S; min(S) and max(S) are minimum and maximum values, respectively, in the fuzzy set S.

Predominant phytochemical of the selected plants (with fuzzy score ≥ 0.5) were identified by extensive literature surge. The three-dimensional structures of all these bioactive molecules as well as the reference drug compound (hydroxychloroquine which is under consideration as a remedy for novel COVID–19 viral disease) were retrieved from PubChem database. Hydrogen atoms were introduced into the ligands structure using Argus lab (4.0.1), so as to customize them for rigid docking. The hydrogenated ligand molecules were then converted into pdb format using Open Babel (2.4) interface (openbabel.org/docs/dev/OpenBabel.pdf), as required for rigid docking. Similarly, 3D structure of standard chemotherapeutic agent (hydroxychloroquine) was also customized for docking (Modi et al., 2013; Chakotiya et al., 2014).

2.4 In silico pharmacokinetic analysis

2.4.1 Drug Likeliness

Drug likeliness of the selected phytoligands (~ 17 compounds) was assessed by using Drug likeness tool DruLiTo, which is an open source virtual screening tool for calculating Lipinski's rule of five, *i.e.,* molecular weight, number of hydrogen bond donors, number of hydrogen bond acceptors and LogP value. Violation of more than one rule would cause exclusion of the said phytochemical. Rest of the selected phytoligands were subjected to ADMETox analysis (Kriszhnamurthi et al., 2018)

2.4.2 ADMETox Analysis

The ADMETox (Absorption, Distribution, Metabolism, Excretion and Toxicity) descriptors of the selected phytocompounds were predicted by conducting admetSAR. The estimation of the probability values of the compounds for diverse profiles including human oral bioavailability, human epithelial colorectal adenocarcinoma cell

(CaCo2) permeability, logP for substrates and inhibitors, predicted aqueous solubility and different toxicity profiles in terms of AMES toxicity and oral toxicity (LC_{50} and LD_{50} values) were computationally predicted. Phytomolecules exhibiting toxic profile as assessed in the *in silico* toxicity analyses were excluded from the study. Rest of the selected phytoligands were subjected to molecular docking analysis (Nisha et al., 2016).

2.5 Molecular Docking and Ligand Receptor Binding analysis

The docking analysis of pdb structures of selected phytoligands (excluding the Lipinski rule and ADMETox violating moieties) with viral receptors (spike glycoprotein, viral nuclease and viral main protease) was carried by Hex Cuda 8.0.0 software. Receptor and Ligand files were imported in the software. The grid dimension of docking was defined according the to the binding site analysis of DoG Site Scorer. Graphic settings and Docking parameters were customized so as to calculate the binding energies (E values) of ligand receptor docking. The parameters used for the docking process were set as (i) Correlation type: Shape + Electro + DARS, (ii) FFT mode: 3D fast lite, (iii) Grid Dimension: 0.7, (iv) Receptor range: 180°, (v) Ligand range: 180°, (vi) Twist range: 360°. The best docked conformations with lowest docking energy were selected for further MD simulations using Pose View for creating pose depictions of selected ligand-receptor binding (Harika et al., 2017).

3. Results And Discussion

3.1 Selection of viral virulence factors

On the basis of the keyword hits scoring results, weightage was given to various parameters selected for screening of herbal leads with respect to antiviral activity. Weightage was decided according to the percentage relevance obtained for each parameter, as given in *Table 1.* Highest percentage relevance was obtained for viral spike glycoprotein inhibitor, followed by other parameters like viral endonuclease inhibitor and viral protease inhibitor. Docking studies were hence performed with these viral receptors, namely, SARS-CoV–2 spike glycoprotein (S2), viral nuclease (NSP15 endoribonuclease) and protease (Main Protease 3CLpro).

3.2 Quality assessment of viral virulence factors

The first quality assessment of the selected viral virulence factors (SARS-CoV–2 spike glycoprotein S2, viral NSP15 endoribonuclease and main protease 3CLpro) was carried out using Ramachandran plot analysis computed with ProCheck. The analysis showed that residues of SARS-CoV–2 spike glycoprotein S2, viral NSP15 endoribonuclease and main protease 3CLpro in the most favorable region were 84%, 93.1% and 89.6%, respectively. Moreover, in the additionally allowed regions, nearly 15.9%, 6.9%and 9.6%residues of SARS-CoV–2 spike glycoprotein S2, viral NSP15 endoribonuclease and main protease 3CLpro were found, respectively. The total quality G-factor of the modeled viral receptors suggested that all of them exhibited favourable stereo-chemical parameters and hence, the 3D structures of all these viral receptors correspond to high-probability conformation for molecular docking. The ProCheck stereo-chemical analysis also showed no bad contacts and scores for main-chain or side-chain parameters. The detailed secondary structural investigation of theSARS-CoV–2 spike glycoprotein S2with PDB sum server revealed that 313 (10.77%) residues were in strands, 2112 (72.70%) residues were in α-helices, 78 (2.68%) residues were in β-turns and 402 (13.83%) residues were in other conformations. Similarly, PDB sum secondary structure of NSP15 endoribonuclease revealed that 72 (10.34%) residues were in strands, 577 (82.90%) residues were in α-helices, 4 (0.57%) residues were in β-turns and 43 (6.17%) residues were in other conformations. Moreover, PDB sum secondary structure of main protease 3CLpro revealed that 75 (12.66%) residues were in strands, 457 (77.19%) residues were in α-helices, 7 (1.18%) residues were in β-turns and 53 (8.95%) residues were in other conformations (*Figure 2).*. Thus,

the above analysis suggests that the backbone conformation and non-bonded interactions of all the selected viral receptors were found to be within reasonable range and hence can be processed for further docking analysis (Kumar et al., 2011).

3.3 Active site analysis of viral receptors

Active site analysis of SARS-CoV–2 spike glycoprotein (S2), viral nuclease (NSP15 endoribonuclease) and protease (Main Protease 3CLpro) as conducted by DoG Site Scorer indicated that there are various active pockets within the studied viral virulence factors with druggability ranging from 0.12 to 0.86 (*Table 2).*. It was found that pockets P_11 (Drug score: 0.847), P_1 (Drug score:0.860) and P_0 (Drug score: 0.805) were energetically favourable for performing further molecular docking studies with the viral receptors being spike glycoprotein, NSP15 endoribonuclease and Main Protease 3CLpro, respectively. While conducting the active site analysis, the DoG Site Scorer tool analysed the heavy atom coordinates on the surface of the 3D structure of the respective viral receptors. Depending on these atomic coordinates, a hypothetical grid was spanned by outruling the chances of any spatial overlap of the grid with the heavy atoms. Furthermore, the tool engages in applying a Gaussian filter to the defined grids, so as to identify spherical pockets of binding. Druggability score (0–1) of the selected spherical pockets are deduced on the basis of their surface area, volume, enclosure and hydrophobicity. As a general rule, higher druggability score is indicative of a more druggable pocket (Volkamer et al., 2012).

3.4 Selection of herbals as promising anti-SARS-CoV–2 candidates

Extensive literature surge combined with a matrix based analysis was conducted for selection of plants having probable utility against SARS-CoV–2. The parameters for selecting the herbals included - a) ethnopharmacological importance of the plant; b) prior pharmaco-therapeutic investigations of the plant; and c) symptomatic relief providing capabilities of the plant. Binary, weightage and fuzzy score analyses were conducted for all the plants so as to screen out herbals exhibiting probable anti-SARS-CoV–2 activity. Plants showing positive assessment for more than 03parameters, reported in PubMed search engine (n = first 20 hits) were selected for further *in silico* analysis. The rationale for selected plants along with their binary, weightage and fuzzy scores has been explained in *Table 3.* Predominant phytocompounds of the selected herbs were also identified by literature surge and the respective chemical structures were retrieved from PubChem database (Chakotiya et al., 2014).

3.5 Pharmacokinetic descriptors of phytoligands

Drug likeliness characteristics of the bioactive phytoligands were assessed by employing a step-wise filtering strategy, wherein various physiochemical properties such as log P, H-bond acceptor, H-bond donor, molecular weight, acidic groups, aromatic rings, number of rotatable bonds and chains, number of hydrogen bonds and molar refractivities were predicted so as to evaluate the drug like behavior of the phytoligand. According to the Lipinski's rule, a drug like moiety should have a low molecular weight (≤ 500 D), log P value ≤ 5, number of hydrogen bond acceptors ≤10, and number of hydrogen bond donors ≤5. A bioactive druggable molecule should ensue to at least 4 of the 5 Lipinski rules (Zhang & Wilkinson, 2007). The Lipinski scores for the selected phytomolecules were found to be within acceptable ranges as elucidated in *Table 4.*

3.6 ADMETox prediction of phytoligands

The results of admetSAR prediction showing the probability values are summarized in *Table 5.* The phytoligands violating any of the ADMETox descriptors (amentoflavone, butenolide, malic acid, β-myrcene, paeoniflorin) were excluded at this step itself. Rest of the phytoligands (~ 12 moieties) did not exhibit any mutagenic or toxic profile.

Based on the predicted probability values, the selected phytoligands were known to get absorbed efficiently by the intestinal epithelium as the values for CaCo2 permeability and intestinal absorption were found to be within permissible range (~ absorption value ≥ 0.5). Such predicted absorption values suggest that the selected phytoligands may get easily transported after getting absorbed in the human body. The aqueous solubility of the selected phytoligands was also predicted to be acceptable (logS ≥ - 4). Moreover, all the selected phytoligands also exhibited efficient binding with the plasma protein, thereby ensuring efficient distribution of the probable drug moieties (Plasma protein binding value ≥ 0.5). As far as metabolism is concerned, inhibition predictions for cytochrome P450 (CYP3A4) super family were conducted. None of the selected phytomolecules exhibited any inhibition of CYP3A4, thus ensuring proper drug metabolism and no excessive drug accumulation as well as toxicity. Most of the selected drugs also exhibited P-glycoprotein modulation activity (~ P-glycoprotein activation value ≥ 0.5), thereby mediating active transport and metabolism of the drug moieties. Other toxicity and excretion characteristics also suggested that the selected phytoligands did not exhibit any signs of oral toxicity (~ acute oral toxicity value ≥ 1.0 Kg/mol) and mutagenicity (Ames mutagenicity value ≥ 0.5), thus making the respective phytoligands as probable lead molecules (Nisha et al., 2016).

3.7 Molecular Docking analysis

Docking results of the viral virulence factors, namely, spike glycoprotein, NSP15 endoribonuclease and Main Protease 3CLpro; and the selected phytoligands (~ 12 phytomolecules) are shown in *Table 6.* These docking based E values have also been compared with that of the standard drug, *i.e.,* hydroxychloroquine. Hex based docking results revealed that the E-value of docking of gamma-glutamyl-S-allylcysteine and salvianolic acid with all the selected viral receptors (viral main protease 3CLpro, spike glycoprotein and NSP15 endoribonuclease) was significantly better as compared to hydroxychloroquine. Several other phytoligands also showed comparable binding energies with respect to at least one of the viral receptors; however, none of the other phyto-moieties exhibited holistic docking abilities. Hence, it is obvious from the E-values that gamma-glutamyl-S-allylcysteine and salvianolic acid bind spontaneously and irreversibly to all the tested viral receptors, thereby blocking the spread and replication of the novel COVID–19 virus. Moreover, the binding efficiency of gamma-glutamyl-S-allylcysteine has been found to be exceedingly better than that of salvianolic acid. Such significant binding affinity of gamma-glutamyl-S-allylcysteine and salvianolic acid presumably indicates the probable mechanism of action of these phytomolecules as viral protease, spike glycoprotein and endoribonuclease inhibitors. Such efficient binding energy of these herbal moieties indicates them to be comparable with that of hydroxychloroquine which has been proposed as the cornerstone for COVID–19 therapy.

Viral spike glycoprotein is required for initiating the attachment and entry of virus into the host cell. Moreover, viral protease is fundamental for continuing the viral life cycle of SARS-CoV–2 as it is required by the virus to catalyze the cleavage of viral polyprotein precursors which are ultimately necessary for viral capsid formation and enzyme production (Anand et al., 2003). Similarly, viral endonucleases are necessary for catalyzing the processing of viral RNAs and hence are required for enduring the process of viral replication (Balkrishna et al., 2020). Henceforth, gamma-glutamyl-S-allylcysteine and salvianolic acid contingently inhibits the entry of SARS-CoV–2 and also inactivates the viral protease as well as endoribonuclease, thereby inhibiting the process of viral capsid formation and replication altogether. Earlier studies have also indicated that gamma glutamyl cysteine ester derivatives could inhibit the HIV–1 gene transcription, wherein, it probably restrained the oxygen free radical-mediated activation of the nuclear factor-kappa B (NF-κB). Moreover, this moiety has a longer plasma life, bioavailability and membrane permeability, thereby making it a suitable drug candidate with sustained antiviral action (Kubota et al., 1998).

3.8 Phytoligand and Viral receptor binding pose depictions

The best docked conformations with lowest docking energy, *i.e.,* gamma-glutamyl-S-allylcysteine and salvianolic acid were selected for further MD simulations using Pose View for creating pose depictions of selected ligand-receptor binding. Upon assessing the binding pose and electrostatic bridging interactions, it was found that only gamma-glutamyl-S-allylcysteine (Herbal source: *Allium sativum)* was able to fit into the active binding pockets of the viral receptors, whereas, salvianolic acid could not establish an irreversible and spontaneous bond with the viral receptors. The orientational binding of gamma-glutamyl-S-allylcysteine and the viral receptors showing the pose view and residue interactions have been depicted in *Figure 3.* It was observed that the amide group of gamma-glutamyl-S-allylcysteine formed a hydrogen bond with the amide residue of glutamine amino acid (1071^{st} position) found in the viral spike glycoprotein. Chemical bridging of gamma-glutamyl-S-allylcysteine and glutamic acid residues of viral endoribonuclease present a similar case where glutamic acid residues (45^{th} position) were invariably bound and neutralized, thereby possibly neutralizing the COVID–19 virus. In earlier studies it has been found that mutation or any change in the glutamine or glutamic acid residues of Ebola virus spike glycoprotein causes viral neutralization (Reynard & Volchkov, 2015). Similarly, the hydroxyl group of gamma-glutamyl-S-allylcysteine formed a hydrogen bond with carbonyl group of proline amino acid (108^{th} position) of viral main protease. Previous studies have also suggested that the proline amino acid residues found in the conserved domains of HIV viral infectivity factor (Vif) are therapeutic targets for neutralizing the human immunodeficiency virus (Ralph et al., 2020). In conclusion, the binding interactions of gamma-glutamyl-S-allylcysteine with viral main protease, spike glycoprotein and endoribonuclease suggest it to be a promising drug candidate for mitigating novel Coronavirus infection.

4. Conclusion

The novel Coronavirus infection accounts for innumerable deaths worldwide, and there is yet no approved prophylactic vaccine or specific treatment available. Based on evidence from laboratory, animal and clinical studies, Hydroxychloroquine is one of the treatment options selected in 'Solidarity'- an international clinical trial to help find an effective treatment for COVID–19, launched by the World Health Organization and partners. However, the repurposed drug, hydroxychloroquine may cause adverse drug reactions and contraindications including cardiomyopathy, fulminant hepatic failure, vertigo and other allergic reactions. Under such circumstances, there is an urgent need for screening novel natural leads that exhibit specific antiviral activities against SARS-CoV–2. The present study suggested that phytoligands derived from medicinal herbs exhibited potential binding properties toward major SARS-CoV–2 virulence factors. Selected phytomolecules were further screened on the basis of acceptable pharmacokinetic and drug-like properties, thereby making them safely exploitable for Coronavirus mitigation system. The current study showed that gamma-glutamyl-S-allylcysteine (GGA) specifically exhibited the most significant binding energy and docking pose toward the major viral virulence factors ($E\ value_{GGA + spike\ glycoprotein} = -578.57$ Kcal/mol; $E\ value_{GGA + viral\ main\ protease} = -493.53$ Kcal/mol; $E\ value_{GGA + endoribonuclease} = -825.00$ Kcal/mol) in comparison with the known chemical moiety hydroxychloroquine($E\ value_{HCQ + spike\ glycoprotein} = -207.47$ Kcal/mol; $E\ value_{HCQ + viral\ main\ protease} = -235.48$ Kcal/mol; $E\ value_{HCQ + endoribonuclease} = -213.54$ Kcal/mol). Hence, the current study provides implication toward the possible usage of gamma-glutamyl-S-allylcysteine (Herbal source: *Allium sativum)* as a novel and prospective drug candidate. This phytomolecule is also found in other species of the *Allium* genus (*A. cepa* and *A. schoenoprasum).*. In view of the current viral pandemic and dearth of effective therapy, further studies should be urgently undertaken so as to explore the therapeutic potential of gamma-glutamyl-S-allylcysteine against SARS-CoV–2.

Abbreviations

ACE2: Angiotensin converting enzyme 2; ADMETox: Adsorption, Distribution, Metabolism, Toxicity; AP–1: Activator protein 1; ATF–2: Activating transcription factor 2; CoV: Coronavirus; COVID: Coronavirus disease; DARS: Decoys as Reference State; DoG: Difference of Gaussian; FFT: Fast Fourier Transform; GGA: Gamma-glutamyl-S-allylcysteine; GPCR: G-protein coupled receptor; HCQ: Hydroxychloroquine; IRF: Interferon regulatory factor; MERS: Middle East Respiratory Syndrome; NF-Kβ: Nuclear Factor kappa-light-chain (β); NSP: Non structural protein; O. E. C. D.: Organisation for Economic Co-operation and Development; PDB: Protein Data Bank; QSAR: Quantitative Structure Activity Relationship; RCSB: Royal Collaborative Structural Biology; SARS: Severe Acute Respiratory Syndrome; TPSA: Total polar surface area; VIF: Viral infectivity factor

Declarations

Author Contributions

AB and RKS conceived the presented research. PT, SS and SND analyzed the information, generated the artwork, and co-wrote the manuscript. AB, NS and RKS investigated and supervised the findings of the work. RKS provided critical revision of this article, and approved the manuscript for submission. All authors agreed with the final version of this manuscript.

Funding

No external funding has been received.

Ethics Statement

The authors confirm that the ethical policies of the journal, as noted on the journal's author guidelines page, have been adhered to. No ethical approval was required as this is an *in silico* study.

Conflict of Interest

The authors declare that the research was conducted in the absence of any commercial or financial relationships that could be construed as a potential conflict of interest.

Acknowledgments

The authors are grateful to Swami Ramdev Ji for institutional research facilities and supports. Authors gratefully acknowledge the efforts of colleagues of Patanjali Research Institute for their help in data collection and processing. We are also thankful to Mr. Gagan Kumar and Mr. Lalit Mohan for their swift administrative supports and encouragements.

Data Availability Statement

All data generated or analysed during this study are included in this published article.

References

Anand K, Ziebuhr J, Wadhwani P, Mesters J R, & Hilgenfeld R. Coronavirus main proteinase (3CLpro) structure: basis for design of anti-SARS drugs. Science 2003; 300: 1763–67. doi: https://doi.org/10.1126/science.1085658

Ang L, Lee HW, Choi JY, Zhang J, Lee MS. Herbal medicine and pattern identification for treating COVID–19: a rapid review of guidelines. Integr Med Res 2020; 9: 100407- 31.https://doi.org/10.1016/j.imr.2020.100407

Balkrishna A, Thakur P, Singh S, Dev S, Jain V, Varshney A, & Sharma R. Glucose antimetabolite 2-Deoxy-D-Glucose and its derivative as promising candidates for tackling COVID–19: Insights derived from in silico docking and molecular simulations. Authorea (Preprint). 2020 (cited 2020, Mar 31). doi.org/10.22541/au.158567174.40895611

Carlos WG, Dela Cruz CS, Cao B, Pasnick S, Jamil S. Novel Wuhan (2019-nCoV) coronavirus. Am J Respir Crit Care Med 2020; 201: P7–8.https://doi.org/10.1164/rccm.2014P7

Chakotiya AS, Chawla R, Tomar M, Thakur P, Goel R, Narula A, Arora R, Sharma RK. In silico herbal bioprospection targeting multi-drug resistant Pseudomonas aeruginosa. Int J Interdiscip Multidiscip Stud 2014; 2:163–76.

Chen N, Zhou M, Dong X, Qu J, Gong F, Han Y, Qiu Y, Wang J, Liu Y, Wei Y, Yu T. Epidemiological and clinical characteristics of 99 cases of 2019 novel coronavirus pneumonia in Wuhan, China: a descriptive study. The Lancet 2020; 395: 507–13.https://doi.org/10.1016/S0140–6736 (20)30211–7

Cucinotta D, Vanelli M. WHO declares COVID–19 a pandemic. Acta Biomed: Atenei Parmensis 2020; 91: 157–60.

Cyranoski D. Mystery deepens over animal source of coronavirus. Nature 2020; 579: 18–9.https://doi.org/10.1038/d41586–020–00548-w

Guan Y, Zheng BJ, He YQ, Liu XL, Zhuang ZX, Cheung CL, Luo SW, Li PH, Zhang LJ, Guan YJ, Butt KM. Isolation and characterization of viruses related to the SARS coronavirus from animals in southern China. Science 2003; 302: 276–8.https://doi.org/10.1126/science.1087139

Guerriero G, Berni R, Muñoz-Sanchez JA, Apone F, Abdel-Salam EM, Qahtan AA, Alatar AA, Cantini C, Cai G, Hausman JF, Siddiqui KS. Production of plant secondary metabolites: Examples, tips and suggestions for biotechnologists. Genes 2018; 9: 309–31. https://doi.org/10.3390/genes9060309

Guo YR, Cao QD, Hong ZS, Tan YY, Chen SD, Jin HJ, Tan KS, Wang DY, Yan Y. The origin, transmission and clinical therapies on coronavirus disease 2019 (COVID–19) outbreak-an update on the status. Mil Med Res 2020; 7:1–10.https://doi.org/10.1186/s40779–020–00240–0

Harika MS, Renukadevi V, Bhargavi S, Karishma S, Abbinaya L, Ramya L, Subhhashini P. Virtual Screening Identifies New Scaffolds for Testosterone 17β-Dehydrogenase (NADP+) Inhibitor. J Chem Pharm Res 2017; 9:134–8.

Hu Z, Yang Z, Li Q, Zhang A, Huang Y. Infodemiological study on COVID–19 epidemic and COVID–19 infodemic. Preprints (Preprint). 2020 (cited 2020 Apr 13). Available from: https://www.preprints.org/manuscript/202002.0380/v2

Huang C, Wang Y, Li X, Ren L, Zhao J, Hu Y, Zhang L, Fan G, Xu J, Gu X, Cheng Z. Clinical features of patients infected with 2019 novel coronavirus in Wuhan, China. The Lancet 2020; 395: 497–506.https://doi.org/10.1016/S0140–6736 (20)30183–5

Jo S, Kim S, Shin DH, & Kim MS. Inhibition of SARS-CoV 3CL protease by flavonoids. J Enzyme Inhib Med Chem 2020; 35: 145–151.https://doi.org/10.1080/14756366.2019.1690480

Kim H. Outbreak of novel coronavirus (COVID–19): What is the role of radiologists?. Eur Radiol 2020; 2020: 1–2. https://doi.org/10.1007/s00330–020–06748–2

Kriszhnamurthi J, Hemalatha CN, Aanandhi MV. In silico approach of interaction studies in Bacopa monnieri compounds targeting multi-proteins for Alzheimer's Disease. Res J Pharm Technol 2018; 11: 1522–6.https://doi.org/10.5958/0974–360X.2018.00283.4

Kubota S, Shetty S, Zhang H, Kitahara S, Pomerantz RJ. Novel inhibitory effects of γ-glutamylcysteine ethyl ester against human immunodeficiency virus type 1 production and propagation. Antimicrob Agents Chemother 1998; 42: 1200–6.https://doi.org/10.1128/AAC.42.5.1200

Kumar R, Kumar S, Sangwan S, Yadav IS, Yadav R. Protein modeling and active site binding mode interactions of myrosinase-sinigrin in Brassica juncea-An in silico approach. J Mol Graph Model 2011; 29: 740–6.https://doi.org/10.1016/j.jmgm.2010.12.004

Lefkowitz EJ, Dempsey DM, Hendrickson RC, Orton RJ, Siddell SG, Smith DB. Virus taxonomy: the database of the International Committee on Taxonomy of Viruses (ICTV). Nucleic Acids Res 2018; 46: D708–17.https://doi.org/10.1093/nar/gkx932

Liu C, Zhou Q, Li Y, Garner LV, Watkins SP, Carter LJ, Smoot J, Gregg AC, Daniels AD, Jervey S, Albaiu D. Research and development on therapeutic agents and vaccines for COVID–19 and related human coronavirus diseases. ACS Central Sci 2020; 6: 315–331. https://doi.org/10.1021/acscentsci.0c00272

Modi V, Mathur N, Pathak AN. Molecular Docking Studies of anti-HIV drug BMS–488043 derivatives using HEX and GP120 Interaction Analysis using Pymol. Int J Sci Res 2013; 3(6):1–7.

Nisha CM, Kumar A, Vimal A, Bai BM, Pal D, Kumar A. Docking and ADMET prediction of few GSK–3 inhibitors divulges 6-bromoindirubin–3-oxime as a potential inhibitor. J Mol Graph Model 2016; 65:100–7.https://doi.org/10.1016/j.jmgm.2016.03.001

Ou X, Liu Y, Lei X, Li P, Mi D, Ren L, Guo L, Guo R, Chen T, Hu J, Xiang Z. Characterization of spike glycoprotein of SARS-CoV–2 on virus entry and its immune cross-reactivity with SARS-CoV. Nat Commun 2020; 11:1–2.https://doi.org/10.1038/s41467–020–15562–9

Qin T, Liu TY, Zhang XD, Chen Z, Ma WY, editors. A study of relevance propagation for web search. Proceedings of the 28th annual international ACM SIGIR conference on Research and development in information retrieval; 2005 Aug 15–19; Salvador, Brazil: ACM Digital Publication; 2005. p. 408–15.https://doi.org/10.1145/1076034.1076105

Ralph R, Lew J, Zeng T, Francis M, Xue B, Roux M, Ostadgavahi AT, Rubino S, Dawe NJ, Al-Ahdal MN, Kelvin DJ. 2019-nCoV (Wuhan virus), a novel Coronavirus: human-to-human transmission, travel-related cases, and vaccine readiness. J Infect Dev Ctries 2020; 14: 3–17. https://doi.org/10.3855/jidc.12425

Reynard O, Volchkov VE. Characterization of a novel neutralizing monoclonal antibody against Ebola virus GP. J Infect Dis 2015; 212:S372–8. https://doi.org/10.1093/infdis/jiv303

Roser M, Ritchie H, Ortiz-Ospina E. Our World in Data: Coronavirus Disease (COVID–19)-Statistics and Research (Internet). 2020 (cited 2020 Mar 14). Available from: https://ourworldindata.org/coronavirus

Senathilake KS, Samarakoon SR, Tennekoon KH. Virtual screening of inhibitors against spike glycoprotein of SARS-CoV–2: a drug repurposing approach. Preprints (Preprint). 2020 (cited 2020 Apr 13). Available from: https://www.preprints.org/manuscript/202003.0042/v2.

Sun P, Lu X, Xu C, Sun W, Pan B. Understanding of COVID-19 based on current evidence. J Med Virol 2020; 2020: 1–4.https://doi.org/10.1002/jmv.25722

Thakur P, Chawla R, Narula A, Goel R, Arora R, Sharma RK. In vitro bactericidal activity of Berberis aristata extract against clinical isolates of Carbapenem-resistant Escherichia coli. J Altern Complement Med 2016; 13: 229–37.https://doi.org/10.1515/jcim–2015–0066

Tripp RA, Tompkins SM. Roles of Host Gene and Non-coding RNA Expression in Virus Infection. Switzerland: Springer; 2018.https://doi.org/10.1007/978–3–030–05369–7

Volkamer A, Kuhn D, Rippmann F, Rarey M. DoGSiteScorer: a web server for automatic binding site prediction, analysis and druggability assessment. Bioinformatics 2012; 28: 2074–5. https://doi.org/10.1093/bioinformatics/bts310

Wang M, Li M, Ren R, Brave A, van der Werf S, Chen EQ, Zong Z, Li W, Ying B. International expansion of a novel SARS-CoV–2 mutant. medRxiv (Preprint). 2020 (cited 2019 Jan 1). Available from: https://www.medrxiv.org/content/10.1101/2020.03.15.20035204v1

World Health Organization (Internet). WHO, Rolling updates on Coronavirus disease- COVID 19. 2020 (cited 2020 Apr 10). Available from: https://www.who.int/emergencies/diseases/novel-coronavirus–2019/events-as-they-happen

Yang L, Wen KS, Ruan X, Zhao YX, Wei F, Wang Q. Response of plant secondary metabolites to environmental factors. Molecules 2018; 23: 762–788. https://doi.org/10.3390/molecules23040762

Yeo C, Kaushal S, Yeo D. Enteric involvement of coronaviruses: is faecal-oral transmission of SARS-CoV–2 possible?. Lancet Gastroenterol Hepatol 2020; 5: 335–7.https://doi.org/10.1016/S2468–1253 (20)30048–0

Zakaryan H, Arabyan E, Oo A, Zandi K. Flavonoids: promising natural compounds against viral infections. Arch Virol 2017; 162: 2539–51.https://doi.org/10.1007/s00705–017–3417-y

Zaki AM, Van Boheemen S, Bestebroer TM, Osterhaus AD, Fouchier RA. Isolation of a novel coronavirus from a man with pneumonia in Saudi Arabia. N Engl J Med 2012; 367:1814–20.https://doi.org/10.1056/NEJMoa1211721

Zhang MQ, Wilkinson B. Drug discovery beyond the 'rule-of-five'. Curr Opin Biotechnol 2007; 18: 478–88. https://doi.org/10.1016/j.copbio.2007.10.005

Zhang T, Wu Q, Zhang Z. Probable Pangolin Origin of 2019-nCoV Associated with Outbreak of COVID–19. Curr Biol 2020; 30: 1346–1351.https://doi.org/10.1016/j.cub.2020.03.022

Zhou F, Yu T, Du R, Fan G, Liu Y, Liu Z, Xiang J, Wang Y, Song B, Gu X, Guan L. Clinical course and risk factors for mortality of adult in patients with COVID–19 in Wuhan, China: a retrospective cohort study. The Lancet 2020; 395: 1054–1062.https://doi.org/10.1016/S0140–6736 (20)30566–3

Tables

Table 1. Selection of COVID-19 virulence factors on the basis of relevance score as assessed by keyword hits scoring matrix

Parameter	Rationale of selection	Total No. of Hits (N)	Hits Screened (n)	Relevant Hits (r)	Percentage Relevance†	Relevance Score§
Viral Spike Glycoprotein inhibitor	Enveloped viruses enter cells by viral glycoprotein-mediated binding (Viral spikes – S proteins) to host cells and subsequent fusion of virus and host cell membranes (Liu et al., 2020).	20	20	18	90	1
Viral Endoribonuclease inhibitor	Endoribonuclease catalyses the processing and degradation of both cellular and viral RNAs, thus determining the amount and functionality of specific RNA molecules in a cell at any given time. It degrades the host mRNA, while cleaves the precursor viral RNAs to produce active genetic material (Balkrishna et al., 2020).	103	20	13	65	0.58
Viral Protease inhibitor	Viral proteases are enzymes encoded by the genetic material of viral pathogens so as to catalyse the cleavage of specific peptide bonds in viral polyprotein precursors or in cellular proteins. The protease cleaves the precursor viral polyprotein to produce functional proteins and enzymes (Jo et al., 2020).	1516	20	12	60	0.5
Anti-bronchitis Herb	Coronavirus causes respiratory illnesses. Hence, herbs providing symptomatic relief against respiratory symptoms might prove to be beneficial (Carlos et al., 2020).	551	20	9	45	0.25
Anti-gastroenteritis Herb	Coronavirus also causes gastroenteritis. Thus, herbs providing symptomatic relief against gastrointestinal ailments might prove to be beneficial (Chen et al., 2020).	52	20	8	40	0.16
Interferon regulatory herb	Interferons (IFNs) are cytokines which are used for communication between cells to trigger the protective defense of the immune system that help eradicate pathogens, Coronavirus in this case (Balkrishna et al., 2020).	952	20	6	30	0

Due to technical limitations, table 2 is only available as a download in the supplemental files section.

Table 3. Selected Herbal moieties showing probable antiviral utility as assessed by employing extensive literature surge.

Plant Source§	Predominant phytocompound	Activity explored†			Binary Score	Weightage Score	Fuzzy Score*	Probable antiviral utility	Ref
		S2	NSP 15	3CL pro					
Alisma canaliculatum A.Braun & C.D.Bouché	Alisol A 24-Acetate	+	−	−	2	1.16	0.46	Anti-influenza activity observed as the herbal moiety inactivates the hemagglutinin spike receptor.	1
Allium cepa L.	Allicin	+	+	+	3	1.66	0.66	Hinders virus attachment to host cell, alter transcription and translation of viral genome in host cell and also affect viral assembly.	2
Allium sativum L.	Gamma-Glutamyl-S-allylcysteine	+	+	+	6	2.49	1	Acts as protease inhibitor mainly.	3
Artemisia capillaris Thunb.	Beta-caryophyllene	+	−	+	5	1.91	0.76	Symptomatic alleviation in case of hepatitis virus infection.	4
Artemisia caruifolia Buch. - Ham. ex Roxb.	Caruilignan	+	−	+	3	1.25	0.5	Anti-influenza and anti-herpes simplex virus activity; also inhibits HIV-1 protease.	5, 6
Asparagus racemosus Willd.	Isoasparagine	−	−	−	3	0.40	0.3	Symptomatic alleviation in case of herpes virus infection.	7
Berberis aristata DC.	Berberine	+	−	+	5	1.91	0.76	Inhibits enterovirus 71 entry and replication by downregulating the MEK/ERK signaling pathway and autophagy.	8
Boswellia serrata Roxb.	11-keto-beta-boswellic acid	+	−	+	3	1.66	0.66	Inhibits Chikungunya and Vesicular stomatitis virus infections by blocking their entry.	9
Camellia sinensis (L.) Kuntze	Quercetin	+	−	+	5	1.91	0.76	Suppressed Hepatitis C virus entry, and also inhibited viral RNA replication.	10
Chlorophytum borivilianum Santapau & R.R. Fern.	Neotigogenin	−	−	−	2	0.40	0.3	Cytokine modulating potential.	11
Curcuma longa L.	Curcumin	+	−	+	5	1.91	0.76	Inhibits entry of Chikungunya and Vesicular stomatitis virus.	9

Plant Source§	Predominant phytocompound	Activity explored†			Binary Score	Weightage Score	Fuzzy Score*	Probable antiviral utility	Ref
		S2	NSP 15	3CL pro					
Epimedium flavum Stearn	Wushanicariin	+	−	−	1	1	0.4	Induced the secretion of type I IFN and pro-inflammatory cytokines.	12
Gingko biloba L.	Amentoflavone	+	−	+	4	1.66	0.66	Inhibits viral protease, specifically in case of HIV infection.	13
Houttuynia cordata Thunb.	β-myrcene	+	−	+	5	1.91	0.76	Inactivation of 3C-like proteinase of murine Coronavirus and dengue virus.	14
Melissa officinalis L.	Citronellal	+	+	−	5	1.49	0.59	Inhibition of HIV-1 protease.	15
Ocimum tenuiflorum L.	Carvacrol	−	−	+	3	0.75	0.35	Inactivation of viral protease in case of HIV infection.	16
Paeonia lactiflora Pall.	Paeoniflorin	+	−	−	3	1.41	0.56	Inhibits viral entry in case of Influenza virus infection.	17
Phyllanthus amarus Schumach. & Thonn.	Gallotannin	−	+	+	5	1.49	0.59	Halts the process of viral replication in case of Herpes simplex virus infection.	18
Rheum rhabarbarum L.	Malic acid	+	−	+	4	1.91	0.76	Inhibits viral entry by ceasing the endosomal fusion in case of influenza virus.	19
Salvia miltiorrhiza Bunge	Salvianolic acid	−	+	+	5	1.49	0.59	Inhibition of HIV-1 integrase and protease.	20
Taxillus sutchuenensis var. *duclouxii* (Lecomte) H.S.Kiu	Butenolide	+	−	+	2	1.5	0.60	Inhibition of Hepatitis C viral NS3 serine protease and ceasing viral entry.	21
Tinospora cordifolia (Willd.) Hook.f. & Thomson	Tinosporaside	+	+	+	5	2.49	1	Immunomodulatory activity; Anti-HIV activity wherein it acts as viral ribonuclease inhibitor.	22
Withania somnifera (L.) Dunal	Withanolide	+	+	+	3	1.41	0.56	Disrupts interactions between viral S-protein receptor binding domain and Host ACE2 receptor.	23
Zingiber officinale Roscoe	6-Gingerol	−	+	+	5	1.49	0.59	Inhibits Hepatitis C virus protease.	24

§Plants are selected on the basis of extensive literature surge, specifically focusing on their ethno-medicinal attributes, symptomatic relief provision abilities and direct/indirect antiviral activity, if any.
†Symbols of + and – denote the presence and absence of viral virulence factor inhibitory properties in the given plant, as deduced on the basis of keyword search matrix analysis using PubMed search engine.
*Fuzzy score μS= (S-minS)/ (maxS-minS), wherein shaded cells represent the ligands selected for further study with a fuzzy score > 0.5.

Table 4. Physicochemical properties of phytoligands in comparison with the standard chemotherapeutic agent.

Ligand/ Standard	Physicochemical Properties				
	Mol. Wt. (≤ 500 D)	Log P (≤ 5)†	H-Bond Donor (≤ 5)	H-Donor Acceptor (≤ 10)	Lipinski violations (if any)*
Allicin	162.02	0.237	0	1	0
Amentoflavone	538.09	2.030	6	10	1
Berberine	336.12	2.473	0	4	0
Beta-caryophyllene	204.19	6.044	0	0	1
11-keto-beta-boswellic acid	470.34	8.131	2	4	1
Butenolide	84.02	0.308	0	2	0
Citronellal	154.14	3.591	0	1	0
Curcumin	368.13	1.945	2	6	0
Gallotannin	1700	9.537	25	46	4
Gamma-Glutamyl-S-allylcysteine	290.09	-2.68	4	7	0
6-Gingerol	294.18	2.437	2	4	0
Malic acid	134.02	-1.474	3	5	0
β-myrcene	136.13	4.170	0	0	0
Paeoniflorin	480.16	-0.464	5	11	1
Quercetin	302.04	1.834	5	7	0
Salvianolic acid	494.12	2.898	7	10	1
Tinosporaside	492.20	0.54	4	10	0
Withanolide	470.27	3.263	2	6	0
Hydroxychloroquine	335.88	4.00	4	2	0

†Logarithm of compound partition coefficient between *n*-octanol and water.

*Shaded cell indicates phytoligand with more than 1 Lipinski violations and hence is eliminated at this stage itself.

Table 5. ADMETox values of phytoligands in comparison with the standard chemotherapeutic agent.

Ligand/ Standard	Absorption		Distribution		Metabolism		Excretion	Toxicity
	Caco-2 permeability (value ≥ 0.5)	Human intestinal absorption (value ≥ 0.5)	Plasma Protein binding (value ≥ 0.5)	Water solubility (logS ≥ -4)	P-glyco-protein activator (value ≥ 0.5)	CYP3A4 inhibition (value ≥ 0.5)	Acute oral toxicity (Kg/mol) (value ≥ 1.0)	Ames test (value ≥ 0.5)
Allicin	0.58 (+)	0.91 (+)	0.50 (+)	-0.89 (+)	0.98 (+)	0.92 (-)	1.935 (-)	0.61 (-)
Amentoflavone	0.87 (+)	0.98 (+)	1.11 (+)	-3.36 (+)	0.44 (-)	0.61 (-)	1.822 (-)	0.68 (-)
Berberine	0.94 (+)	0.77 (+)	0.83 (+)	-2.97 (+)	0.68 (+)	0.58 (-)	1.545 (-)	0.75 (-)
Beta-caryophyllene	0.86 (+)	0.98 (+)	0.83 (+)	-4.68 (+)	0.89 (+)	0.86 (-)	2.366 (-)	0.99 (-)
11-keto-beta-boswellic acid	0.54 (+)	0.99 (+)	1.05 (+)	-3.45 (+)	0.63 (+)	0.79 (-)	2.834 (-)	0.82 (-)
Butenolide	0.76 (+)	0.96 (+)	0.096 (-)	0.23 (+)	0.98 (+)	0.98 (-)	1.976 (-)	0.77 (-)
Citronellal	0.92 (+)	0.97 (+)	0.70 (+)	-2.44 (+)	0.98 (+)	0.96 (-)	2.307 (-)	0.99 (-)
Curcumin	0.76 (+)	0.97 (+)	0.83 (+)	-3.36 (+)	0.59 (+)	0.53 (-)	1.992 (-)	0.96 (-)
Gamma-Glutamyl-S-allylcysteine	0.92 (+)	0.63 (+)	0.50 (+)	-1.68 (+)	0.93 (+)	0.74 (-)	1.648 (-)	0.55 (-)
6-Gingerol	0.59 (+)	0.99 (+)	0.85 (+)	-3.23 (+)	0.89 (+)	0.59 (-)	2.290 (-)	0.57 (-)
Malic acid	0.95 (+)	0.77 (+)	0.23 (-)	0.27 (+)	0.98 (+)	0.90 (-)	0.844 (+)	0.87 (-)
β-myrcene	0.77 (+)	0.96 (+)	0.43 (-)	-3.44 (+)	0.98 (+)	0.66 (-)	1.660 (-)	0.92 (-)
Paeoniflorin	0.82 (+)	0.41 (-)	0.67 (+)	-2.97 (+)	0.65 (+)	0.85 (-)	3.502 (-)	0.53 (-)
Quercetin	0.64 (+)	0.98 (+)	1.17 (+)	-2.99 (+)	0.91 (+)	0.69 (-)	2.559 (-)	0.90 (-)
Salvianolic acid	0.93 (+)	0.96 (+)	1.03 (+)	-3.20 (+)	0.65 (+)	0.83 (-)	2.069 (-)	0.58 (-)
Tinosporaside	0.84 (+)	0.83 (+)	0.50 (+)	-3.65 (+)	0.54 (+)	0.75 (-)	3.236 (-)	0.70 (-)
Withanolide	0.62 (+)	0.97 (+)	1.18 (+)	-4.00 (+)	0.51 (+)	0.85 (-)	3.660 (-)	0.78 (-)
Hydroxy-chloroquine	0.66 (+)	0.99 (+)	0.86 (+)	-4.00 (+)	0.84 (+)	0.83 (-)	2.684 (-)	0.70 (-)

*Denoted '+' or '-' sign relates to the presence or absence of a predicted activity, respectively. Shaded cells indicate the descriptors violating the standard values, thereby excluding the respective phytoligand(s) from further studies.

Due to technical limitations, table 6 is only available as a download in the supplemental files section.

Figures

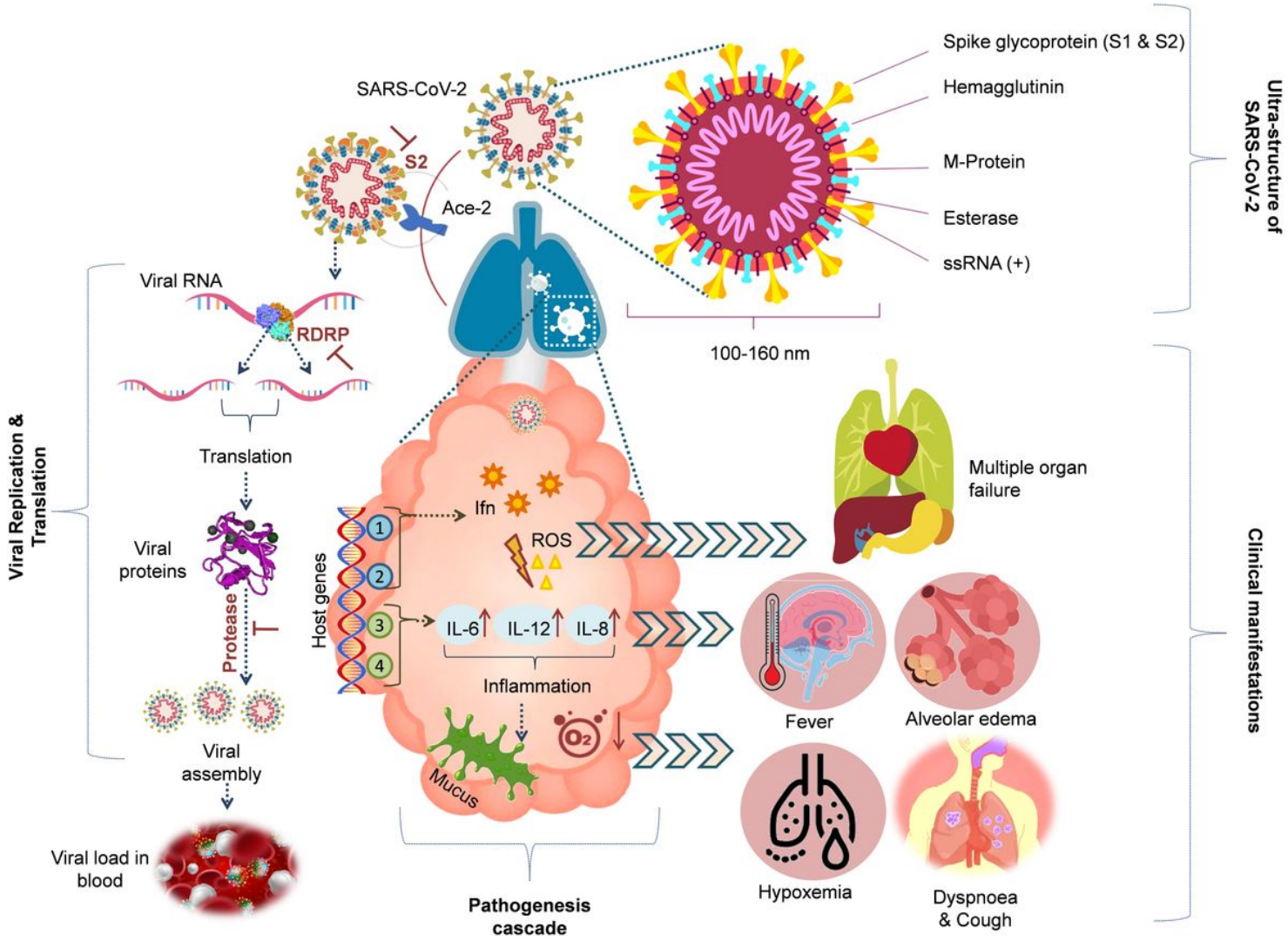

Figure 1

Molecular Pathogenesis & Clinical manifestations of Novel Coronavirus (SARS-CoV-2). SARS-CoV-2 infects lung parenchymal cells and its entry is facilitated by binding of viral envelope glycoprotein (S2) with host ACE2 receptor. Upon entering the host bronchial cells, the virus elicits an immunological response as mediated by host genes, namely, TLRs-dependent IFN induction pathways [IRF-3/7 (1) & NF-Kβ (2)] and myeloid-differentiation primary response 88 pathways [ATF-2 (3) & AP-1 (4)]. Subsequently, inflammatory cytokines (IL-6, IL-12 and IL-8), interferon gamma and reactive oxygen species (ROS) are produced. These inflammatory and oxidation mediators activate a pathogenesis cascade, leading to inflammation, alveolar mucus formation and decrease in partial pressure of oxygen in bronchioles. Simultaneously SARS-CoV-2 gets hold of host metabolic machinery and initiates its replication and translation, as mediated by the primary viral virulence factors (RNA dependent RNA polymerase/ endoribonuclease, and viral main protease). As a consequence, viral load in blood increases (viraemia), ultimately leading to serious clinical manifestations including fever, alveolar edema, hypoxemia, dyspnoea, cough and multiple organ failure.

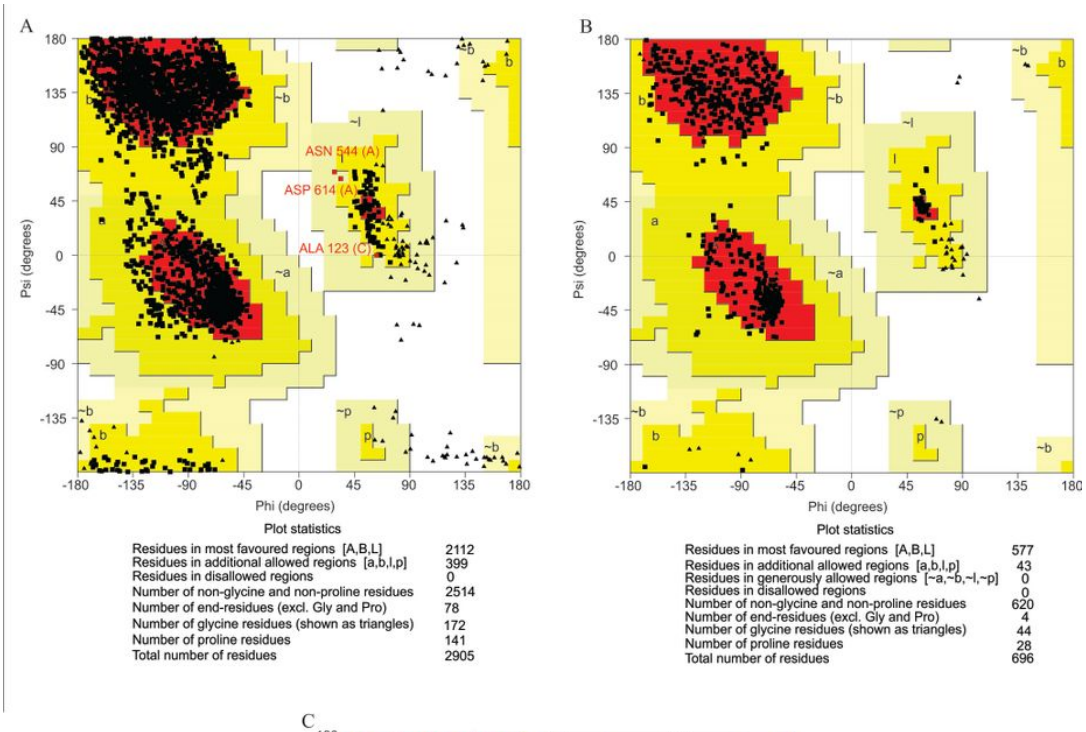

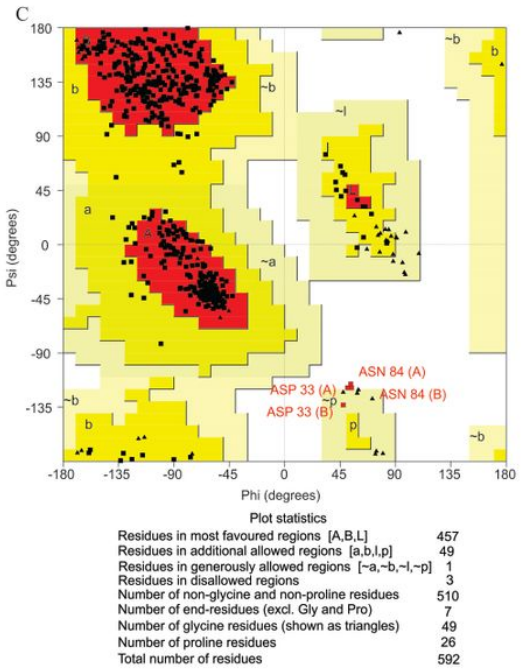

Figure 2

Ramachandran plot of the structure models of SARS-CoV-2 receptors - (A) Spike glycoprotein, (B) NSP15 endoribonuclease, and (C) Main protease 3CLpro. The most favoured regions are coloured in red and marked as A, B, and L. The additionally allowed regions are coloured in yellow and marked as a, b, l, and p. All non-glycine and proline residues are shown as filled black squares, whereas glycine residues (non-end) are shown as filled black triangles. Disallowed residues, if any are represented by white colour. Abbreviations: Asn: asparagine; Asp: aspartate; Gly: glycine; Pro: proline.

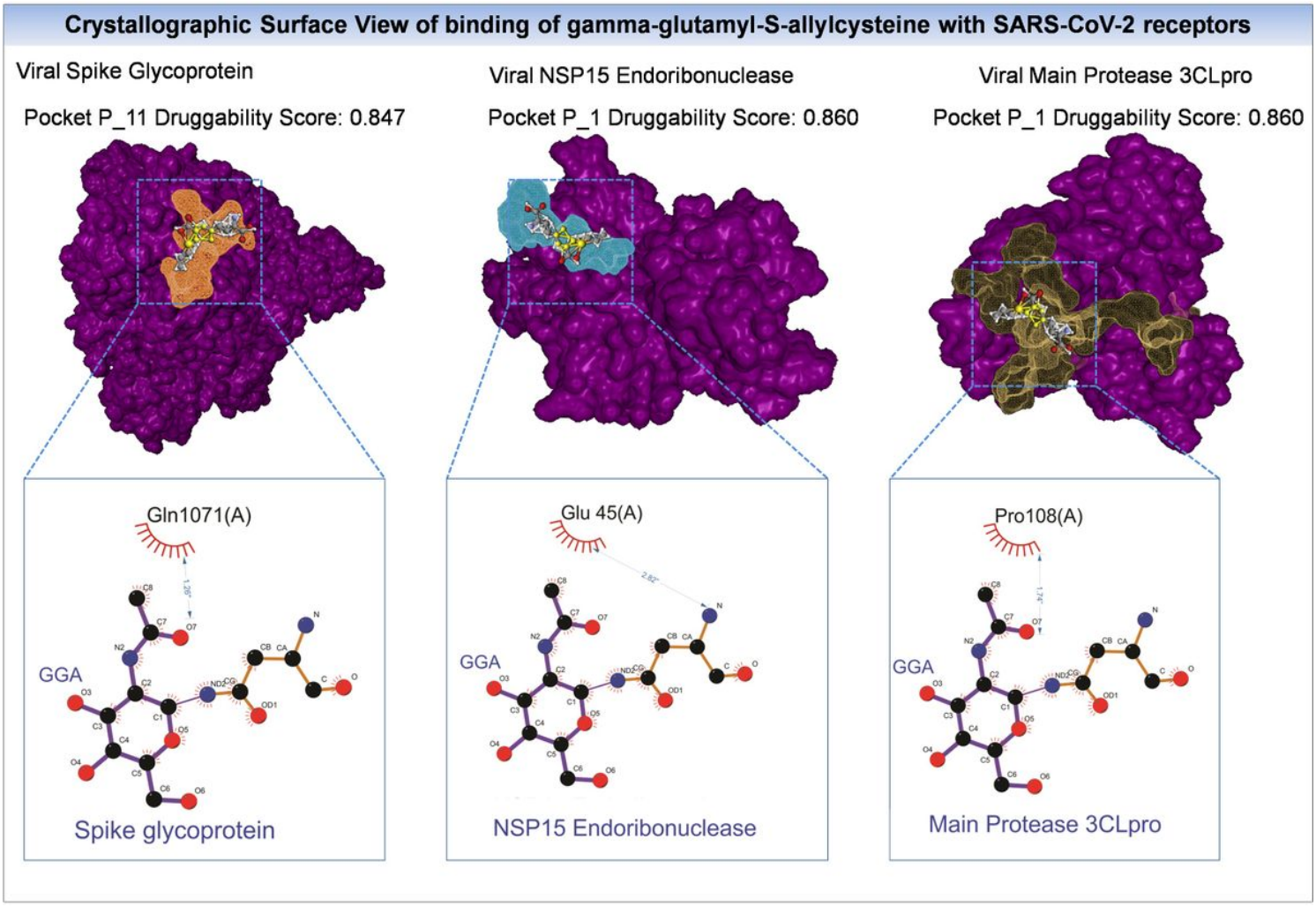

Figure 3

Binding pose depictions of gamma-glutamyl-S-allylcysteine as probable drug candidates targeting SARS-CoV-2 receptors Amide group of gamma-glutamyl-S-allylcysteine (GGA) formed a hydrogen bond with the amide residue of glutamine amino acid (1071st position) of the viral spike glycoprotein. Glutamic acid residues (45th position) of viral endoribonuclease showed irreversible interaction with GGA. Additionally, the hydroxyl group of GGA formed a hydrogen bond with carbonyl group of proline amino acid (108th position) of viral main protease 3CLpro.

Supplementary Files

This is a list of supplementary files associated with this preprint. Click to download.

- Table2.docx
- Table6.docx
- GraphicalAbstract.jpg